CONTRACT NO. NASw-144
NK-6929

No.13

Effect of NUCLEAR RADIATION on Materials at CRYOGENIC TEMPERATURES

LNP Quarterly Report to NASA

JAN 1964-
MAR. 1964

LOCKHEED NUCLEAR PRODUCTS

ER-6929

QUARTERLY PROGRESS REPORT No. 13

January 1964 through March 1964

Effect of Nuclear Radiation on materials at Cryogenic Temperatures

PREPARED UNDER

National Aeronautics/Space Administration Contract NASw-114

APPROVED BY

C. A. Schwarzberk

NASA CRYOGENICS
PROJECT MANAGER

Lockheed-Georgia Company

LOCKHEED
NUCLEAR
PRODUCTS

A Division of Lockheed Aircraft Corporation

If this document is supplied under the requirements of a United States Government contract, the following legend shall apply unless the letter U appears in the coding box:

This data is furnished under a United States Government contract and only those portions hereof which are marked (for example, by circling, underscoring or otherwise) and indicated as being subject to this legend shall not be released outside the Government (except to foreign governments, subject to these same limitations), nor be disclosed, used, or duplicated, for procurement or manufacturing purposes, except as otherwise authorized by contract, without the permission of Lockheed-Georgia Company, A Division of Lockheed Aircraft Corporation, Marietta, Georgia. This legend shall be marked on any reproduction hereon in whole or in part.

The "otherwise marking" and "indicated portions" as used above shall mean this statement and includes all details or manufacture contained herein respectively.

Code: U	Contract: NASw-114

FOREWORD

This quarterly report is submitted to the Office of Space Launch Vehicles of the National Aeronautics and Space Administration in accordance with the requirements of NASA Contract NASw-114.

TABLE OF CONTENTS

LIST OF FIGURES

LIST OF TABLES

1 INTRODUCTION AND SUMMARY

27885

This report describes the progress made on Contract NASw-114 during the first quarter, January through March, of 1964.

The testing of materials for the screening program was continued during this reporting period, both in-pile and out-of-pile.

Room temperature, out-of-pile testing was completed on sets of three tensile and three tensile-notch specimens for each of the alloys added to the screening program after the completion of the major room temperature testing program in December 1962. The results of these tests will provide reference data for the evaluation of irradiation effects on these materials. If rigorous statistical analysis of the test results indicate the necessity, two additional samples of each type are available for room temperature testing to provide a broader background of comparison. The results obtained are reported herein.

In-pile testing, after exposure to an integrated dose of 1×10^{17} nvt fast (> 0.5 Mev) neutrons, was continued using sets of three specimens for each type of alloy and test. These have been completed for four alloys, AISI Types 304 and 347 Stainless Steels and Titanium Alloys 55A and 5% Aluminum, 2-1/2% Tin. The results of these tests are also reported.

In-pile testing has been initiated on several other titanium alloys, but publication of test results will be deferred until the data are more nearly complete.

Temperature correlation and refrigeration control data were obtained from an instrumented aluminum alloy specimen to assure adequate temperature control of aluminum alloy test samples. These, in addition to similar data obtained from instrumented statinless steel and titanium specimens, provide adequate assurance of proper temperature control and the temperature correlation program has now been completed.

Author

Additional flux mapping was accomplished in the test position in HB-2 beam port, using low activation energy foils, to demonstrate the validity of the method used to determine exposure time and accumulated dose for the test specimens. This method was further described in Quarterly Report No. 12.

Modifications to test and ancillary equipment, herein described, were made to improve operational reliability and increase the quantity of useful data generated by the testing program.

2 EQUIPMENT

2.1 TEST LOOPS

Difficulties were encountered during this period with the dynamometer signal from loop 201-002. Two (2) in-pile tests were aborted when the loss of the dynamometer signal resulted in an inability to monitor the applied stress. The first signal loss occurred shortly after an insertion in HB-2 and the test was immediately aborted. The failure of the dynamometer was traced to a water leak in the instrument lines.

Replacement of the dynamometer was handled expeditiously when approval was granted to perform the work with the test loop remaining in the quadrant. The forward, more highly activated portion of the loop was placed in the hot cave for shielding so that when the quadrant water was lowered to the level of the test loop, operators were able to work for reasonable periods in that area. This method of repair saved an inestimable period of time compared to that which would have been required to transfer the test loop to the hot laboratory outside the containment vessel and perform all the work remotely.

The instrumentation lines were leak tested with a helium mass spectrometer before resuming in-pile testing with the test loop. The dynamometer signal was lost the second time during the actual testing of a test specimen in the 11th irradiation exposure of the test loop following the above mentioned repairs.

Moisture, which appeared to be the cause of failure, was removed from the instrument tubes carrying the dynamometer lines by connecting a vacuum pump to the upper end of the tube containing the bundle of instrument lines and evacuating this tube. This resulted in evaporation of the moisture in the lines and an increase in resistance of the signal leads to ground. The dynamometer signal was regained and in-pile testing was continued with the same test loop.

An investigation to determine the cause for a decrease of the signal during the ensuing test resulted in the discovery of a leak in the dynamometer lead instrument tube which must be repaired before using the test loop for additional testing. A procedure for the replacement of the defective tube with new, thoroughly inspected material was submitted to NASA for approval. It is assumed that the repairs will be made during the next reporting period.

Several instances of failure of the small Type A286 stainless steel 12 pt. cap screws, which are used to secure the end plate on the test loop head, were encountered during this period. The point of failure was below the surface of the head assembly which necessitated drilling a hole in the screws by remote techniques prior to the actual screw extraction. These screws failed in torsional shear during removal from the test loop head. The ratio of failure increased as a function of irradiation exposure cycles and appears to be an irradiation induced effect. End cap screws are now being replaced after each five (5) irradiation cycles to prevent the occurrence of extensive irradiation induced embrittlement. On the basis of the limited experience thus far, this corrective action appears to have reduced or eliminated the failure rate.

Prior to the reactor start-up in the last reactor cycle of the operating period, test loop 201-003 sustained some damage when the beam port valve was inadvertently actuated with this test loop stored in the beam port for shielding while Quadrant "D" was drained. The extent of damage is an indentation approximately 1/8" deep on the top of the test loop at a position 12" forward of the area which is in the beam port seal when the test loop is in a "full forward" position. A mock-up of the tube with a simulation of the identation will be made as the first step in repairing the loop. This indentation will be made as the first step in repairing the loop. This indentation will then be repaired with the use of appropriate tooling developed for this purpose. On the basis of the results, a procedure will be submitted to NASA for approval of the repair of the test loop. This repair also will be made in the ensuing period.

2.2 TEMPERATURE CONTROL CALIBRATION

An aluminum alloy (7178-T6) instrumented test specimen was subjected to the three step calibration and correlation procedure which was developed to determine specimen temperature distribution and refrigeration control settings at 30°R. (Reference: Quarterly Report #11, Stainless Steel Instrumented Specimen; and Quarterly Report #12, Titanium Alloy Instrumented Specimen.) It was necessary to demonstrate temperature control for the stainless steel, the titanium alloy and the aluminum alloy specimens due to the magnitude of the difference in thermal conductivity among the alloys.

The initial step in the calibration, as previously reported in Quarterly Report No. 12, Page 5, consisted of the calibration of three thermocouples affixed to the instrumented aluminum specimen at liquid nitrogen temperature and at several temperatures between liquid nitrogen and 30°R obtained by use of the refrigerator. A National Bureau of Standards calibrated platinum resistance bulb was used as a primary standard in this calibration. Figures 1, 2 and 3 are the calibration curves for the three thermocouples. Figure 4 gives the correction factors required to correct the output of each thermocouple to standard reference table emf values. After thermocouple calibration had been completed, the temperature distribution across the specimen was measured at approximately 30°R both out-of-pile and in-pile. The results are shown in Table 1. The temperature spreads are considered acceptable and temperature correlation has now been completed for this program.

2.3 REMOTE HANDLING EQUIPMENT AND SAMPLE CHANGING SYSTEM

2.3.1 Carriage Modification

Modification of the carriage assembly used to drive the test loops into either the reactor beam port or the hot cave was completed during this reporting period. (Reference: Quarterly Report No. 11, Section 2.4, Pages 11-18; and Quarterly Report No. 12,

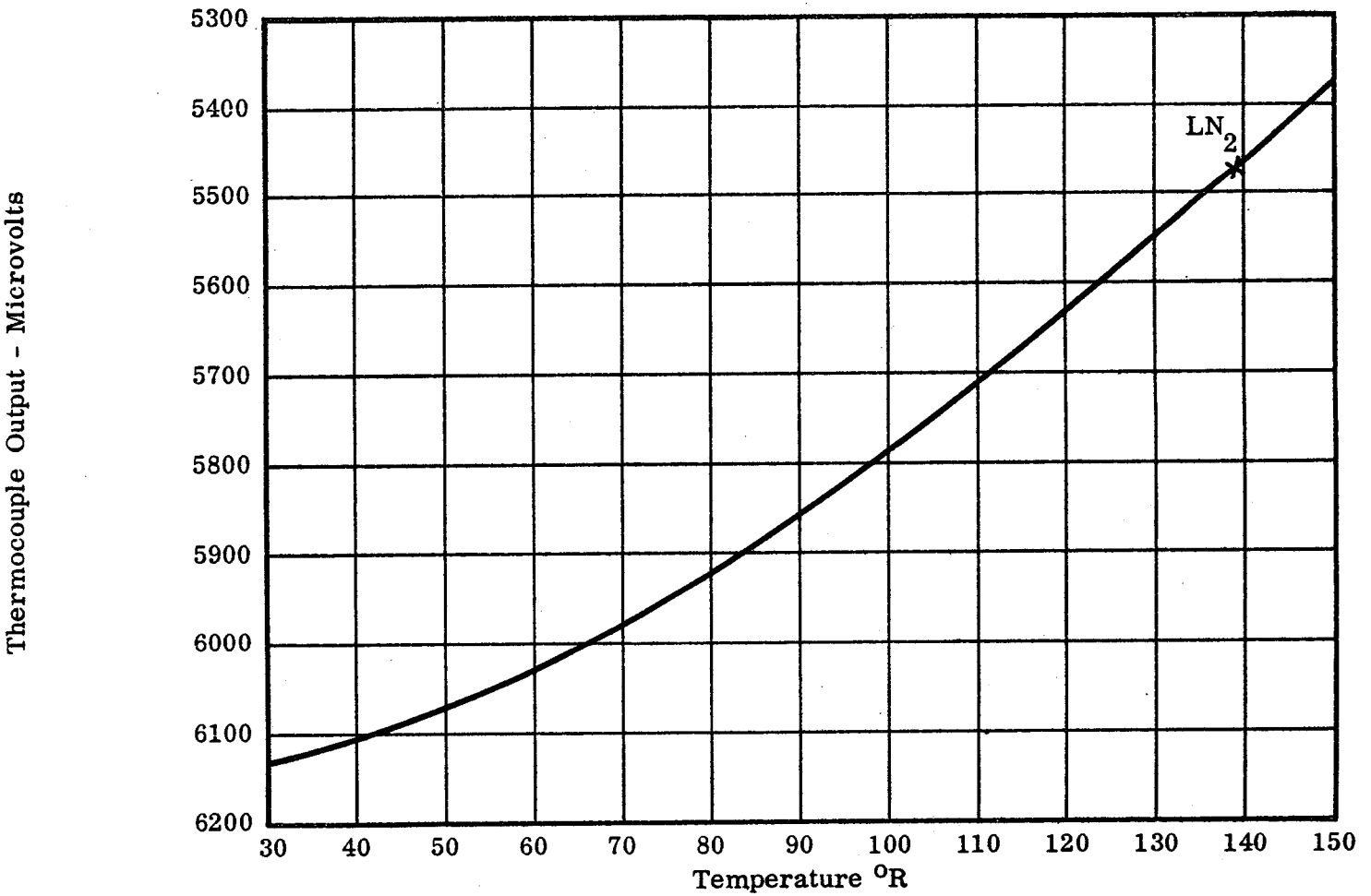

FIGURE 1 ALUMINUM ALLOY (7178-T6) INSTRUMENTED SPECIMEN CALIBRATION CURVE FOR THERMOCOUPLE NO. 1. TEMPERATURE MEASUREMENTS MADE WITH NBS CALIBRATED PLATINUM RESISTANCE BULB STANDARD

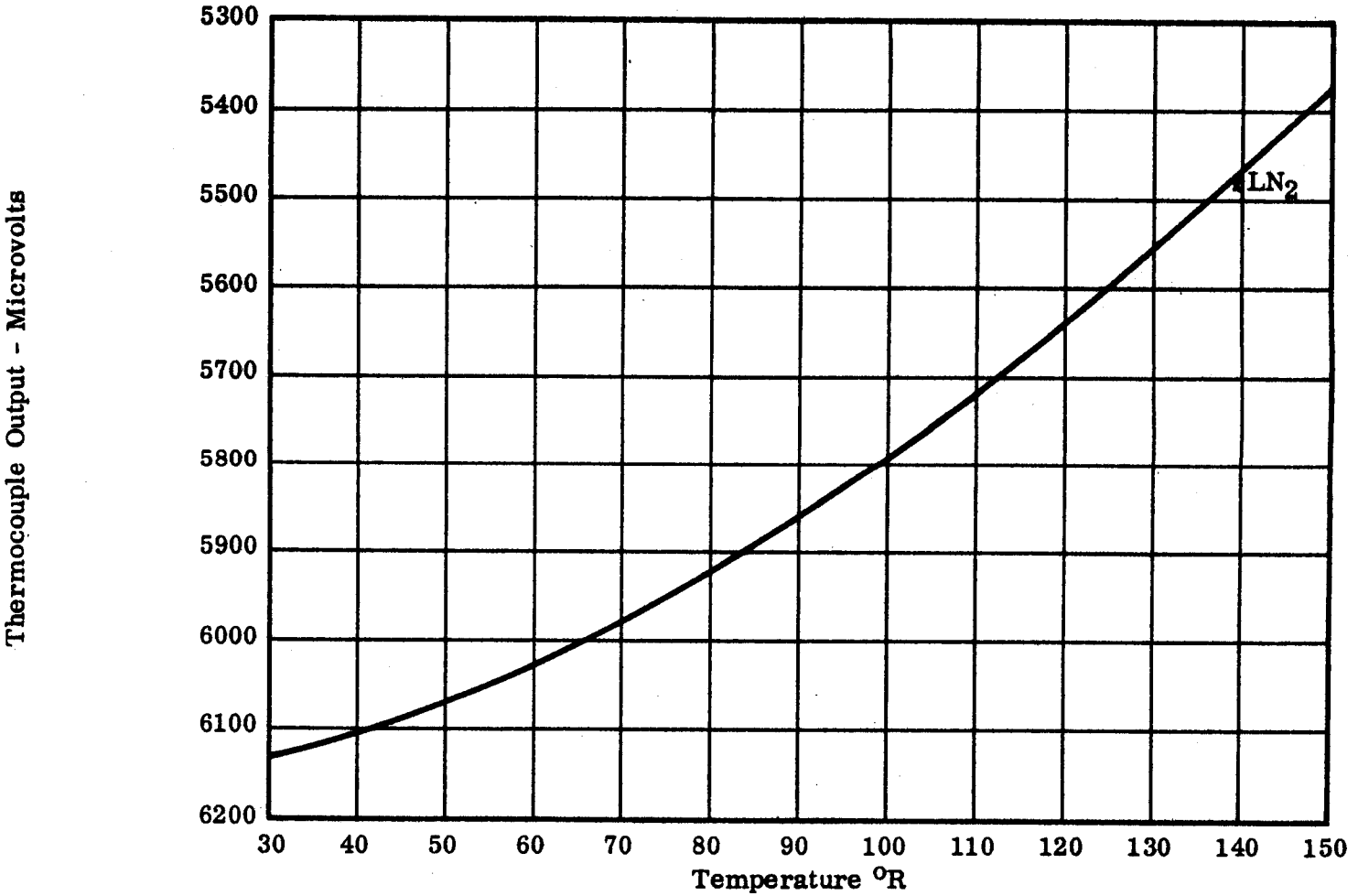

FIGURE 2 ALUMINUM ALLOY (7178-T6) INSTRUMENTED SPECIMEN CALIBRATION CURVE FOR THERMOCOUPLE NO. 2. TEMPERATURE MEASUREMENTS MADE WITH NBS CALIBRATED PLATINUM RESISTANCE BULB STANDARD

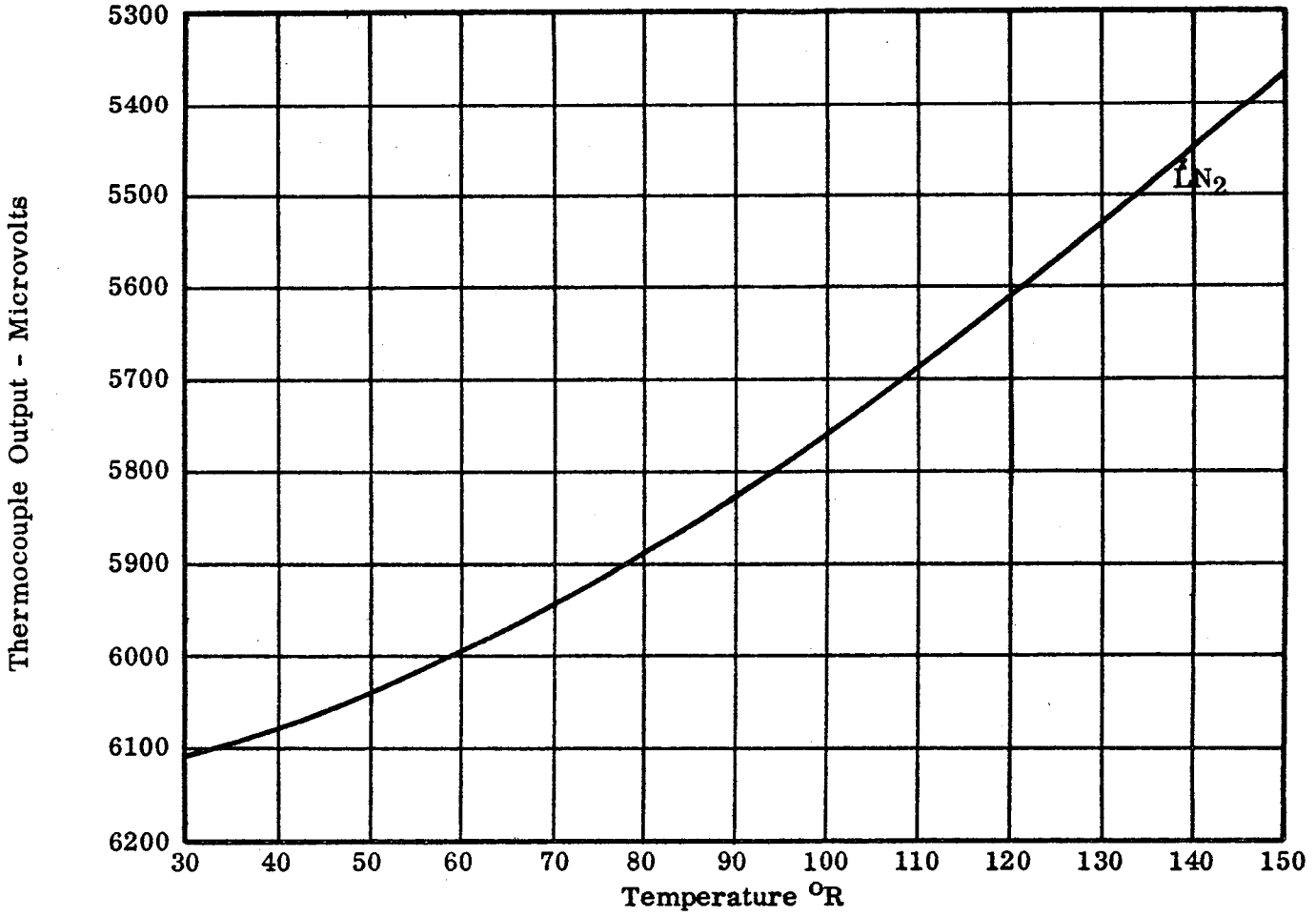

FIGURE 3 ALUMINUM ALLOY (7178-T6) INSTRUMENTED SPECIMEN CALIBRATION CURVE FOR THERMOCOUPLE NO. 3. TEMPERATURE MEASUREMENTS MADE WITH NBS CALIBRATED PLATINUM RESISTANCE BULB STANDARD

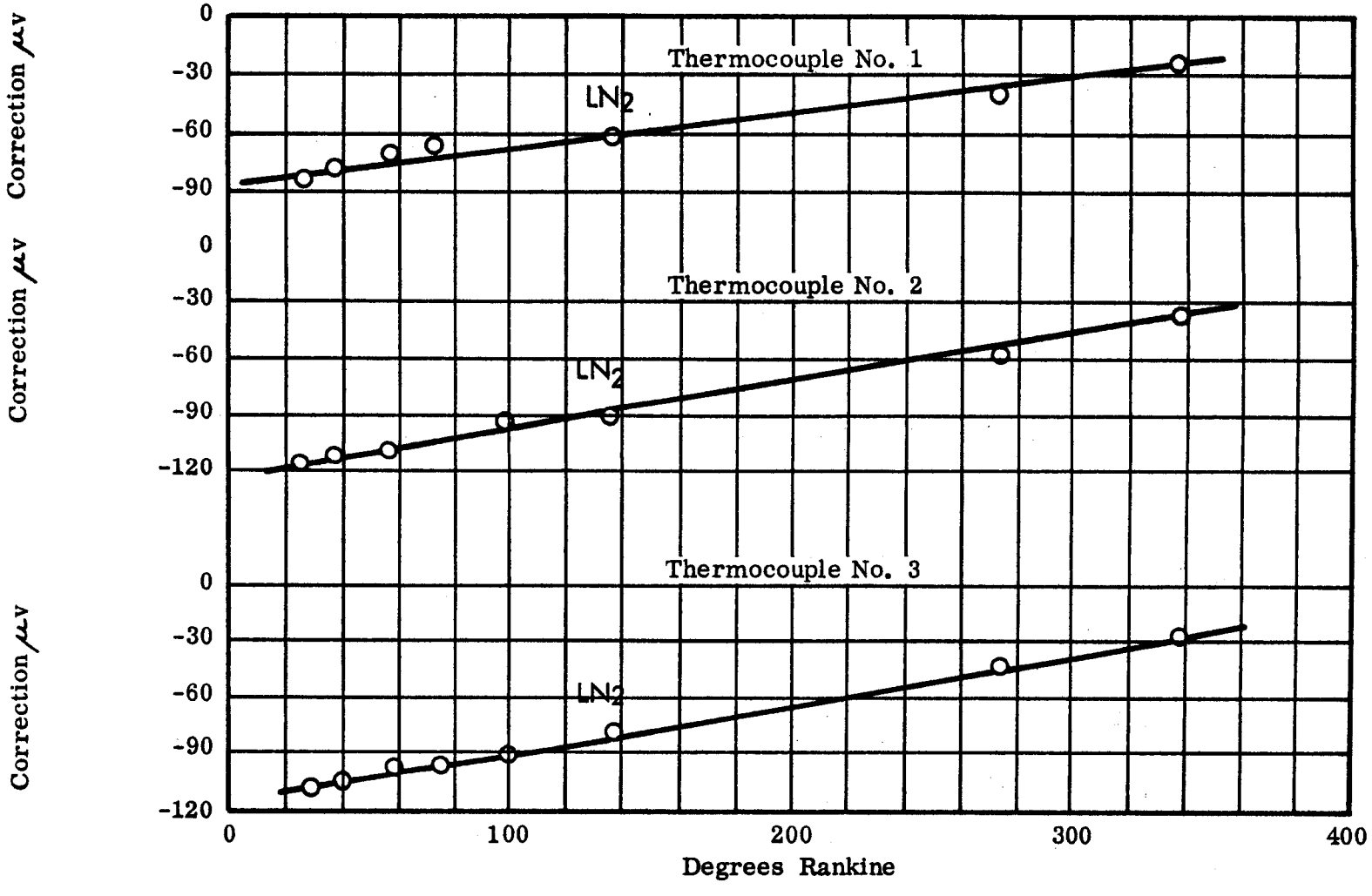

FIGURE 4 CORRECTION FACTORS FOR ALUMINUM INSTRUMENTED SPECIMEN THERMOCOUPLES 1, 2 & 3

TABLE 1

TEMPERATURE DISTRIBUTION, ALUMINUM ALLOY (7178-T651)
INSTRUMENTED SPECIMEN

Thermocouple Number	Position	Indicated Temperature
OUT-OF-PILE		
1	Forward Gage Mark	31.1°R
2	Midpoint Gage Length	29.2°R
3	Aft Gage Mark	29.8°R
Helium Inlet Temperature 27.4°R Helium Outlet Temperature 29.5°R		
IN-PILE		
1	Forward Gage Mark	31.3°R
2	Midpoint Gage Length	29.3°R
3	Aft Gage Mark	31 °R
Helium Inlet Temperature 27.1°R Helium Outlet Temperature 29.6°R		

Section 2.5, Pages 12-13.) The modification consisted essentially of material changes. The cage holding the bearings which serve as wheels and the bracket holding the cage were changed to Inconel X from AISI Type 420 Stainless Steel and AISI Type 304 Stainless Steel, respectively, with such design modifications as were necessary to compensate for the difference in physical properties of the substituted material and increase the overall strength of the structure to withstand the operating stresses.

After the modified design satisfactorily passed the required pre-neutron testing, the carriages were used in operational beam port insertions. A high incidence of service failure was encountered in the outer bearing races fabricated from AISI Type 440C Stainless Steel. The highest failure location was in the right rear outer race position and the failure rate average approximately one race for each ten (10) test loop insertions into the reactor beam port. Examination of the failed races indicated a brittle type of fracture. No anomolies of hardness or structure were observed.

It was concluded that AISI Type 440C had insufficient inherent ductility to provide sufficient local plastic yielding to maintain continuity of deformation during peak point stresses encountered in highly localized areas for times of short duration during bearing rotation under load. The microscopic cracks which developed in place of microscopic plastic flow were propagated at relatively low energy levels, due to the high notch sensitivity of the material, and resulted in the brittle type of failure.

No excessive number of failures was encountered with the inner races, made from the same material with the same heat treatment but given complete internal support by the shaft.

The above considerations made it evident that a change in the outer race material was the logical approach to reduction of the failure rate. Recommendation of an alternate material was requested from the original bearing manufacturer and AISI Type 420 Stainless Steel was suggested. This would provide an increase in tensile elongation from 2% to 8%, accompanied by a reduction in hardness from R_C 60 to R_C 52. A trial set of outer races was fabricated from AISI Type 420 and heat treated to maximum hardness.

It was felt, however, that an increase in ductility and a reduction in notch sensitivity greater than is obtainable in the AISI 400 series martensite stainless steels was desirable. One of the Maraging Steels, 18 Ni (300), with a compressive yield strength of 315,000 psi, and a tensile elongation of 12% at a hardness of R_C 52-54 seemed to offer a desirable combination of mechanical properties for this application.

This material has been reported as susceptable to stress-corrosion cracking in aqueous environments. After discussion of these reports with metallurgists of the International Nickel Company, developers of the Maraging Steels, it was concluded that this phenomenon is at worst a long time occurrence above rather high stress thresholds and it is felt that the material offers promise of greatly increased outer race service life expectancy. A trial set of outer races was fabricated from 18 Ni (300) Maraging Steel and aged for three hours at 900°F.

Bearing cage assemblies were prepared with AISI Type 420 Stainless Steel and with 18 Ni (300) Maraging Steel outer races and installed in the hot laboratory Instron Testing Machine as described in Quarterly Report No. 11, Section 2.4 (pages 16 and 17) using the fixture shown in Figure 9 of that report. Each cage was loaded to 10,000 lbs., the load removed and reloaded to 10,000 lbs. for thirty cycles. One AISI Type 420 Stainless Steel race failed with the initial loading, and testing of this material was discontinued.

A complete set of four cages using 18 Ni (300) races were tested, the bearings were then disassembled and inspected for cracks using Zyglo (ZL-22) penetrant and visually inspected for "Brinelling" of the outer race by the harder AISI Type 440C needle bearings against which the load was sustained. Neither cracks nor "Brinelling" were present. The cages were then reassembled and installed in Carriage No. 3.

A hydraulic cylinder arrangement, described in Quarterly Report No. 11, Section 2.4 (pages 12, 17, Figure 5) was installed on a test loop carriage to simulate the force vectors on the drive assembly encountered in opposing primary coolant pressure during test loop insertion into HB-2. The assembly was driven

against a hydraulic pressure of 1700 psi, or approximately 7000 lb. thrust, for thirty cycles of one foot travel each. The bearings were again disassembled and inspected with Zyglo (ZL-22). No cracks or other defects were noted in any of the 18 Ni (300) outer races.

Approval was then granted by NASA to undergo a pre-neutron procedure consisting of five insertions into HB-2 against primary coolant pressure with the reactor not in operation. This was accomplished without incident late in the reporting period.

After the satisfactory completion of these tests, approval was granted by NASA to use the modified carriage during reactor operations. The modified carriage has been used for three specimen irradiation insertions without incident. The use of this carriage will be continued in the ensuing reporting period. The remaining carriages will also be modified to use 18 Ni (300) Maraging Steel outer races.

2.3.2 Beam Port Valve

The rubber chevron seals in the reactor beam port, which had a tendency to "roll" during test loop insertion, as noted in Quarterly Report No. 12, Section 2.5 (Page 6-13), were replaced with polyurethane seals of a slightly modified shape designed during the previous reporting period. Forty-five (45) insertions have been made into HB-2 since this modification without evidence of seal damage.

The beam port valve seals were tested for damage which may have been caused by the inadvertent closure of the beam port valve on test loop 201-003 or the ensuing removal of the damaged test loop through the seals. The beam port was actuated ten cycles with a test loop in the "through seal" position. Water samples were taken at the face of the valve immediately after valve operation and one hour after valve operation. These samples were analyzed for increased radiation level which would have indicated admixture of primary coolant in the quadrant. No increase in activity in the water was noted and it was concluded that the valve and seals were undamaged.

The design of the auxiliary pumping system for monitoring leakage through the chevron seals at HB-2, discussed in Quarterly Report No. 12, Section 2.5 (Page 14), was completed during this reporting period. Approval for installation was obtained from NASA and the installation is in operation. Insufficient operational experience had been obtained at the end of this reporting period to enable evaluation of the effect of this change on the service life of the 10HP Clevite Pump.

2.3.3 Hot Cave

A high water level alarm was installed in the hot cave during this reporting period. A small but significant quantity of quadrant water is introduced into the hot cave each time a test loop is inserted. The level of this water is controlled by the intermittent operation of a sump pump which transfers it to a hot drain line. Overflow of this water through a hot cave exhaust filter housing into the dry annulus area between the quadrant wall and the containment vessel at the -25 foot level could contaminate the dry annulus.

To prevent such an occurrence, a sight glass and a float level alarm system was installed in the hot cave. The float actuates an audible alarm at the test console at the 0'-0" level when the water in the sump reaches a level of fifteen (15) inches.

2.3.4 Cask and Cart

Pre-neutron procedures and operational check-out of the installation of the cask stand and the cask in Quadrant "D", the insertion of a test loop into the cask, closing the cask and removal of cask and stand from Quadrant "D" were completed during this reporting period. The above were done both with the quadrant drained and with the quadrant filled with water. The cask containing the test loop was transferred to the air lock penetration of the containment vessel and the method of cask and test loop removal without breaking containment was demonstrated.

Design of a drive mechanism to facilitate transfer of the cask and test loop through the airlock vessel penetration was submitted to NASA for approval.

The remote handling stand designed for hot cell use with the test loops was installed in Hot Cell No. 1 for the development of remote major maintenance techniques.

An irradiated test loop, Loop 201-003, was installed in the transfer cask remotely in Quadrant "D" and brought to the 0'-0" level to demonstrate the shielding capability of the cask for the actual test loop geometrical configuration. The test loop had been withdrawn from pile 35 hours and 40 minutes prior to this test, at which time it had a total irradiation exposure of 2.1×10^{18} nvt fast (>.5 Mev) and 6.5×10^{17} nvt thermal neutrons. Readings taken at the "hot" end of the loop showed a 50 mr, 35 mr γ field at contact at the point of maximum mis-match in the mating surfaces of the cask. These acceptably low readings indicate adequate cask shielding and the cask is now approved for storage of an irradiated test loop.

The wheels on the cart were modified and axles were re-bushed with Dyflon bushings, a composite stainless steel and teflon bushing especially designed to bear heavy loads without flow, to facilitate movement of the cask outside the containment vessel. The cart was then used in the pre-neutron check of the transfer equipment. The transfer cask, containing the dummy test loop, was brought through the air lock vessel penetration and placed on the cart. The cart was then placed on a "low-boy" trailer for truck transfer to the hot laboratory area.

In the hot laboratory area, the cask cover was removed and the dummy test loop was removed from the cask using the remote handling tongs. The loop was then placed on a stand positioned on the front of the remotely operable hot cell door for insertion into the hot cell. The dummy test loop was replaced in the cask and the procedure reversed to return the cask and dummy loop to the containment vessel.

2.4 REFRIGERATION SYSTEM

The erratic behavior of the expansion engines in engine pod #1 continued to cause difficulty in the operation of the refrigeration system. A representative of the manufacturer was called in to

assist in the evaluation of the problem. On his recommendation, the crosshead was disassembled, checked and cleaned. A damaged needle bearing on the crank throw was replaced and the unit reassembled.

Two broken piston rods delayed operation of the refrigeration system on two different occasions. The breaks occurred just above the position where the rod is clamped to the crosshead. An investigation revealed that one of these rods was different from other rods in the system. On the end of the piston rod, there is a button or disc which is inserted into a hole in the base of the piston. A spanner type nut is then threaded into the hole in the piston to secure the rod to the piston. It was found that this button was brazed to this particular piston rod, whereas other piston rods are an integrally machined rod and button unit. The manufacturer of the refrigeration system was asked to evaluate the rod failures and suggested that the micro-structure of the Inconel X material may have been altered during the furnace brazing operation, leading to a reduction in mechanical properties. Replacement piston rods have been ordered, specifying that they be of integrally machined construction.

Several pistons were reconditioned with new piston sheaths. The sheaths were fabricated of Textolite, pressed in place, and machined to tolerances commensurate with the cylinder bore. After installing these reconditioned pistons in the expansion engines in engine pod #1 and allowing a "break-in" period of several days, the capacity of the system increased considerably. It is concluded that piston rods and sheaths must be replaced intermittently to ensure satisfactory performance of the system.

The expansion engins in engine pod #2 continued to operate reliably during this reporting period and provided sufficient refrigeration capacity for the continuation of in-pile testing.

3 FLUX MAPPING

Two additional sets of foils were irradiated during this reporting period in Reactor Cycles 10P and 14P. This was done for two reasons; to verify the shape of the knee portion of Figures 7 and 8, Quarterly Report No. 12, and to determine the effect on the flux level in HB-2 of the presence of approximately 2.6 kilograms of nickel plated Mallory 1000 inserted in lattice position LA-5 for Experiment 62-07 after the prior flux mapping had been completed. Since the purpose of these foil runs was to establish the flux level at various rod positions, only the low-activation-energy foils (Np, Th, S and Ni) were used in these foil packages.

The shapes of the spectral curves resulting from these foil runs are similar to those reported in Figures 5 and 6 in Quarterly Report No. 12. The flux levels measured by the Neptunium 237 foils, those with neutron energies greater than 0.75 Mev, are plotted as a function of fuel control rod position and superimposed on the curve reported as Figure 7, Quarterly Report No. 12. These data are presented as Figure 5 of this report.

Examination of Figure 5 shows that the two additional points are in good agreement with the curve. Therefore, the use of the extrapolated curve for neutron energies $>$ 0.50 Mev presented as Figure 6 for dose calculation seems justified within the limits of reasonable experimental error.

Additional Thorium and Sulfur foils were received from Georgia Nuclear Laboratories during this period, and arrangements were made to purchase additional Neptunium foils from the Monsanto Chemical Company. After calibration of the Neptunium foils by the Lockheed-Georgia Nuclear Laboratories, sufficient low-activation-energy foils will be available to permit additional flux level determinations as required to assess the possible effect of additional in-pile experiments on the flux level in HB-2.

Point	Source
1	Neptunium 237 Foil Irradiated in Cycle 10P; January 15, 1964, Reactor Power 42.2 MW
2	Neptunium 237 Foil Irradiated in Cycle 14P; March 185, 1964, Reactor Power 38.9 MW

Reference Figure No. 7, Quarterly Report #12.

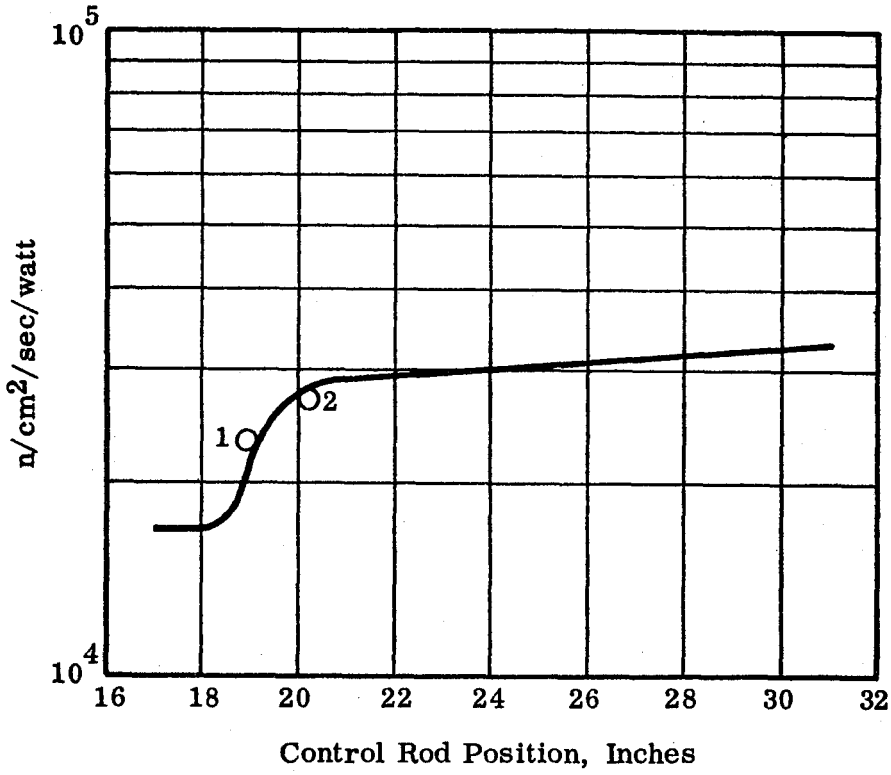

FIGURE 5 FAST NEUTRON FLUX (0.75 Mev) MEASURED WITH Np^{237} FOILS VS. FUEL CONTROL ROD POSITION

Point	Source
1	Foils Irradiated in Cycle 10P, 1937 to 2007, 1/15/64, Reactor Power 42.2 MW
2	Foils Irradiated in Cycle 14P, 0500 to 0530, 3/18/64, Reactor Power 38.9 MW

Reference Figure 8, Quarterly Report No. 12

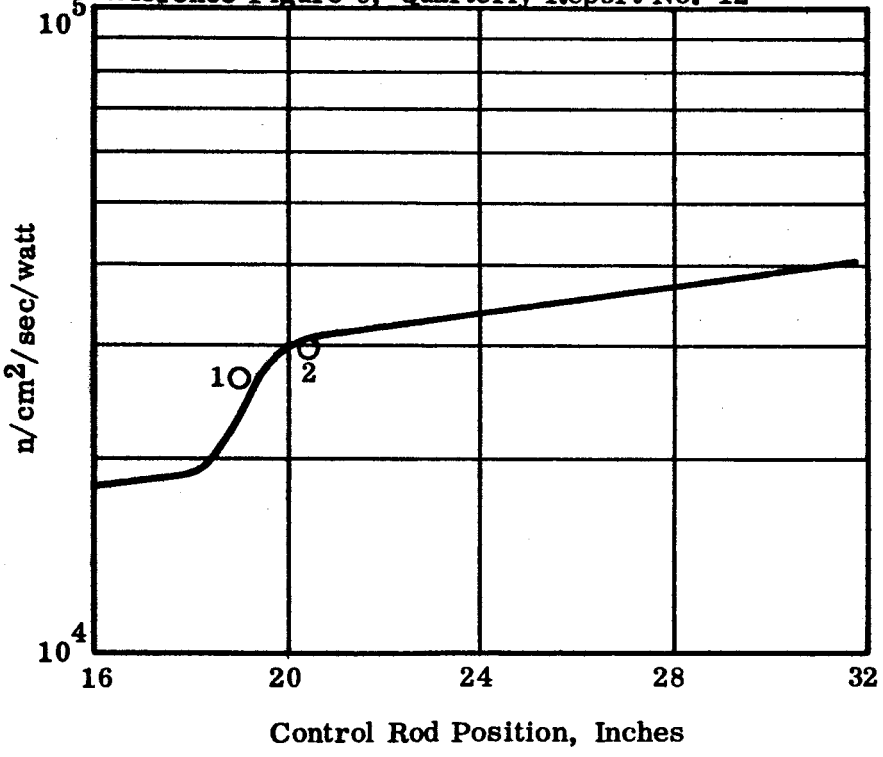

FIGURE 6 FAST NEUTRON FLUX (0.50 MEV), EXTRAPOLATED FROM SPECTRAL CURVES BASED ON Np^{237}, S^{32} AND Ni^{58} FOILS VS. FUEL CONTROL ROD POSITION

4 TEST PROGRAM

4.1 SCREENING TESTS

The room temperature out-of-pile portion of the testing program was resumed during this reporting period. Three tensile and three tensile notch tests were performed on each of the new materials listed in Quarterly Report No. 10 and described in the Addendum to ER-5542, Pedigree of Metals and Alloys, September 1963, to provide reference data for the evaluation of test results on irradiated samples. The results of these tests are given in Tables 2, 3, 4 and 5. In all cases, agreement among the individual tests is well within acceptable limits for tensile testing. If a more critical statistical review indicates that more data is desirable, two additional tests will be run on each material.

In-pile testing was continued during this period. Sets of three tensile and three tensile notch tests have been completed for four materials: Stainless Steel AISI Types 304 and 347 and Titanium Alloys 55A and 5% Aluminum, 2-1/2% Tin. The results of these completed tests are given in Tables 6, 7, 9 and 10, Section 4.3, with a summary of the out-of-pile test results for each alloy given in Table 8, 9 and 10.

In-pile testing has been initiated on several additional alloys: Titanium Alloy 5% Al, 2-1/2% Sn, extra low interstitial content; Titanium Alloy 6% Al, 4% V, in both annealed and aged conditions; and Stainless Steel A286 (AMS 5735). Reporting of the so-far fragmentary results obtained from these tests will be deferred until sets of three tests have been completed for each alloy.

It is planned to complete testing of three specimens for each of the remaining titanium alloys in the ensuing quarter and include a report on these materials in Quarterly Report No. 14.

TABLE 2

OUT-OF-PILE TEST RESULTS, ALUMINUM ALLOYS
TEST TEMPERATURE - ROOM TEMPERATURE

Specimen	Ultimate Tensile Strength, F_{tu} in psi	Tensile Yield Strength, F_{ty} in psi	Elongation in 1/2" (4 Diameters), %	Reduction of Area, %
ALLOY 7079-T6				
Tensile Test				
13 Ba 1	97,730	90,750	12	18
13 Ba 4	97,800	91,100	11	16
13 Ba 6	98,200	91,600	12	17
Average	97,900	91,150	12	17
Scatter	±2.4%	±3.6%	+0, -8	±5.8
Tensile Notch Test				
12 Ba 48	110,000	Notch to Unnotched Ratio		
13 Ba 49	112,100	Avg ÷ Avg 1.13		
13 Ba 51	110,500	Low ÷ High 1.12		
Average	110,800	High ÷ Low 1.14		
Scatter	±1.1%			
ALLOY A 356-T61				
Tensile Test				
14 Ba 85	42,650	31,700	12	17
14 Ba 92	52,500	30,975	18	24
14 Ba 95	44,600	31,250	14	18
Average	46,600	31,300	13.3	19.7
Scatter	±10.5%	●11%	±23%	±18%
Tensile Notch Test				
14 Ba 1	58,400	Notch to Unnotched Ratio		
14 Ba 4	52,000	Avg ÷ Avg 1.16		
14 Ba 16	51,400	Low ÷ High 0.98		
Average	53,900	High ÷ Low 1.37		
Scatter	±6.5%			

TABLE 3

OUT-OF-PILE TEST RESULTS, NICKEL ALLOYS
TEST TEMPERATURE - ROOM TEMPERATURE

Specimen	Ultimate Tensile Strength, F_{tu} in psi	Tensile Yield Strength, F_{ty} in psi	Elongation in 1/2" (4 Diameters), %	Reduction of Area, %
INCONEL X, PRECIPITATION HARDENED				
Tensile Test				
3 Fa 18	200,700	144,000	24	40
3 Fa 20	200,500	139,500	24	42
3 Fa 24	201,750	140,350	24	40
Average	201,000	141,300	24	40
Scatter	±0.25%	±1.6%	Nil	+5, -0
Tensile Notch Test				
3 Fa 49	246,200	Notch to Unnotched Ratio		
3 Fa 50	245,000	Avg ÷ Avg 1.22		
3 Fa 51	246,000	Low ÷ High 1.21		
Average	245,700	High ÷ Low 1.23		
Scatter	±0.25%			

TABLE 4

OUT-OF-PILE TEST RESULTS - STEEL ALLOYS
TEST TEMPERATURE - ROOM TEMPERATURE

Specimen	Ultimate Tensile Strength, F_{tu} in psi	Tensile Yield Strength, F_{ty} in psi	Elongation in 1/2" (4 Diameters), %	Reduction of Area, %
A-286, AMS 5737, 1650° SOLUTION TREATED AND AGED				
Tensile Test				
8 Ca 4	179,000	141,200	23	50
8 Ca 7	174,000	131,400	22	49
8 Ca 37	170,000	136,000	24	52
Average	174,300	136,200	23	50
Scatter	±2.5%	±3.5%	±4.5%	±1.5%
Tensile Notch Test				
8 Ca 9	182,000	Notched to Unnotched Ratio		
8 Ca 11	183,000	Avg ÷ Avg 1.05		
8 Ca 17	184,500	Low ÷ High 1.02		
Average	183,200	High ÷ Low 1.09		
Scatter	±0.7%			
AM 350, SCT				
Tensile Test				
10 Ca 40	193,000	183,000	12	43
10 Ca 42	193,000	182,000	17	60
10 Ca 23	195,500	180,500	14	50
Average	193,600	181,800	14.3	51
Scatter	±0.7%	±0.7%	±18%	±16%
Tensile Notch Test				
10 Ca 1	250,000	Notched to Unnotched Ratio		
10 Ca 12	278,000	Avg ÷ Avg 1.34		
10 Ca 14	253,000	Low ÷ High 1.28		
Average	260,300	High ÷ Low 1.44		
Scatter	±5.4%			

TABLE 4 (Continued)

Specimen	Ultimate Tensile Strength, F_{tu} in psi	Tensile Yield Strength, F_{ty} in psi	Elongation in 1/2" (4 Diameters), %	Reduction of Area, %
AISI TYPE 440C, STAINLESS STEEL, R_C 60				
Tensile Test				
9 Ca 1	322,000	279,000	5	8
9 Ca 2	324,000	281,000	5	7
9 Ca 7	337,000	303,000	3	6
Average	327,700	287,700	4.3	7
Scatter	±2.6%	±4.2%	+16, -30	±14
Tensile Notch Test				
9 Ca 33	186,000	Notched to Unnotched Ratio		
9 Ca 34	189,400	Avg ÷ Avg 0.57		
9 Ca 36	189,000	Low ÷ High 0.55		
Average	188,100	High ÷ Low 0.59		
Scatter	±0.9%			
AUSTENITIC MANGANESE STEEL T-450 ANNEALED				
Tensile Test				
1 Eb 40	111,700	37,200	68	90
1 Eb 43	113,000	36,000	70	90
1 Eb 45	111,500	35,400	70	90
Average	112,000	36,200	69.3	90
Scatter	±0.7%	±2.5%	±1.4%	Nil
Tensile Notch Test				
1 Eb 32	124,400	Notched to Unnotched Ratio		
1 Eb 37	125,000	Avg ÷ Avg 1.12		
1 Eb 39	122,000	Low ÷ High 1.08		
Average	124,000	High ÷ Low 1.12		
Scatter	±1%			

TABLE 4 (Continued)

Specimen	Ultimate Tensile Strength, F_{tu} in psi	Tensile Yield Strength, F_{ty} in psi	Elongation in 1/2" (4 Diameters), %	Reduction of Area, %
TYPE 17-7PH STAINLESS STEEL, RH 950				
Tensile Test				
11 Ca 11	268,000	230,000	16	56
11 Ca 17	268,000	227,700	14	50
11 Ca 20	265,500	236,300	13	46
Average	267,000	231,300	14.3	51
Scatter	± 0.5%	± 1.8%	● 9%	± 10%
Tensile Notch Test				
11 Ca 2	261,000	Notched to Unnotched Ratio		
11 Ca 4	256,000	Avg ÷ Avg 0.99		
11 Ca 7	275,300	Low ÷ High 0.96		
Average	264,100	High ÷ Low 1.04		
Scatter	± 3.7%			

TABLE 5

OUT-OF-PILE TEST RESULTS – TITANIUM ALLOYS
TEST TEMPERATURE – ROOM TEMPERATURE

Specimen	Ultimate Tensile Strength, F_{tu} in psi	Tensile Yield Strength, F_{ty} in psi	Elongation in 1/2" (4 Diameters), %	Reduction of Area, %
5% Al, 2-1/2% Sn, ELI, ANNEALED				
Tensile Test				
8 Aa 4	132,000	118,800	12	40
8 Aa 9	131,000	118,600	18	61
8 Aa 11	129,800	117,500	14	48
Average	130,900	118,300	14.67	49.67
Scatter	±4.5%	±5.5%	±14%	±21%
Tensile Notch Test				
8 Aa 3	164,000	Notched to Unnotched Ratio		
8 Aa 5	154,000	Avg ÷ Avg 1.19		
8 Aa 20	150,000	Low ÷ High 1.14		
Average	156,000	High ÷ Low 1.26		
Scatter	±4.5%			

TABLE 6

TEST RESULTS, STAINLESS STEEL AISI TYPE 304, ANNEALED
TEST TEMPERATURE - 30°R

Specimen	Total Accumulated Fast Neutron Dose (nvt)	Ultimate Tensile Strength (F_{tu} in psi)	Tensile Yield Strength (0.2% offset) (F_{ty} in psi)	Elongation in 1/2" (4 Diameters), %	Reduction of Area, %
TENSILE TEST					
2 Cb 229*	1.82×10^{17}	258,000	53,600	38.6	40
2 Cb 265*	1.89×10^{17}	259,000	52,200	36.3	36
2 Cb 245*	1.92×10^{17}	267,000	53,300	32.5	Not measurable due to fracture shape
Average		261,000	53,000	35.8	38
Scatter		±1.7%	±1.3%	±8	±5.3
TENSILE NOTCH TEST					
2 Cb 292**	1.00×10^{17}	203,000	Notched-Unnotched Ratio		
2 Cb 295**	1.37×10^{17}	157,000			
2 Cb 269**	1.12×10^{17}	220,000	Avg ÷ Avg	0.69	
2 Cb 299	1.00×10^{17}	175,000	Low ÷ High	0.56	
2 Cb 295	1.00×10^{17}	149,000	High ÷ Low	0.85	
Average		181,000			
Scatter		±20%			

* Tensile and yield strength test results reported in Quarterly Report No. 12, Table 2 (Page 24).
** Previously reported in Quarterly Report No. 12, Table 3 (Page 25).

TABLE 7

TEST RESULTS, STAINLESS STEEL AISI TYPE 347, ANNEALED
TEST TEMPERATURE - 30°R

Specimen	Total Accumulated Fast Neutron Dose (nvt)	Ultimate Tensile Strength (F_{tu} in psi)	Tensile Yield Strength (0.2% offset) (F_{ty} in psi)	Elongation in 1/2" (4 Diameters), %	Reduction of Area, %
TENSILE TEST					
4 Cb 39*	2.10×10^{17}	277,000	69,000	39.8	77
4 Cb 43*	1.05×10^{17}	230,000	61,000	38.6	76
4 Cb 44*	0.93×10^{17}	246,000	59,200	41.3	76
Average		251,000	63,000	40.0	76
Scatter		± 9.5%	± 8%	+3, -6	+1, -Nil
TENSILE NOTCH TEST					
4 Cb 27**	1.18×10^{17}	244,000	Notched-Unnotched Ratio		
4 Cb 54**	1.19×10^{17}	265,000	Avg ÷ Avg	0.973	
4 Cb 56	1.00×10^{17}	224,000	Low ÷ High	0.809	
Average		244,300	High ÷ Low	1.152	
Scatter		± 8.37%			

* Tensile and yield strength test results reported in Quarterly Report No. 12, Table 4 (Page 27).
** Previously reported in Quarterly Report No. 12, Table 5 (Page 28).

TABLE 8

TEST RESULTS, AISI 304 STAINLESS STEEL AND AISI 347 STAINLESS STEEL

Test Condition	Ultimate Tensile Strength (F_{tu} in psi)	Tensile Yield Strength		Tensile Notch Strength		Elongation in 1/2" (4 Diameters), %	Reduction of Area, %
		F_{ty} in psi	% of Ultimate Tensile	F_{tu} in psi	% of Unnotched		
SUMMARY OF AVERAGE TEST DATA, STAINLESS STEEL AISI TYPE 304, ANNEALED							
Room Temperature, Unirradiated	95,200	36,800	38.7	106,300	111.7	80	85
30°R, Unirradiated	239,800	42,900	17.80	167,000	70	36	40
30°R, * Irradiated to 1.82×10^{17} nvt	261,000	53,000	20.3	181,000	69	35.8	38
SUMMARY OF AVERAGE TEST DATA, STAINLESS STEEL AISI TYPE 347, ANNEALED							
Room Temperature, Unirradiated	94,400	44,900	47.6	112,900	119.6	58	85
30°R, Unirradiated	237,700	52,200	22	227,000	95	42	75
30°R, * Irradiated to $1\text{-}2 \times 10^{17}$ nvt	251,500	63,300	25	244,300	97.3	40	76

* Overexposure due to lack of accurate flux data at time of test.

TABLE 9

TEST RESULTS, TITANIUM ALLOY 55A, ANNEALED CONDITION

SUMMARY OF TEST RESULTS

Test Condition	Ultimate Tensile Strength (F_{tu} in psi)	Tensile Yield Strength		Tensile Notch Strength		Elongation in 1/2" (4 Diameters), %	Reduction of Area, %
		F_{ty} in psi	% of Ultimate Tensile	F_{tu} in psi	% of Unnotched		
Room Temperature, Unirradiated	66,900	53,600	80	84,300	126	30	58
30°R, Unirradiated	169,200	121,600	72	166,400	98	33	60
30°R, Irradiated to 1×10^{17} nvt	192,800	132,200	68.5	194,200	100.7	*	*

TEST RESULTS, 30° R, IN-PILE

Specimen	Test Condition	Ultimate Tensile Strength (F_{tu} in psi)	Tensile Yield Strength (F_{ty} in psi)	Elongation in 1/2" (4 Diameters), %	Reduction of Area, %
Tensile Test					
1 Aa 144	1×10^{17} nvt	214,300	134,000	*	*
1 Aa 138	1×10^{17} nvt	185,000	132,000	*	*
1 Aa 148	1×10^{17} nvt	179,000	130,500	*	*
Average		192,800	132,200	*	*
Scatter		±9.15%	±1.3%		
Tensile Notch Test					
1 Aa 136	1×10^{17} nvt	197,400	Ratio, Notch-Unnotched		
1 Aa 198	1×10^{17} nvt	195,200			
1 Aa 183	1×10^{17} nvt	190,000	Avg ÷ Avg	1.007	
Average		194,200	Low ÷ High	0.886	
Scatter		±1.9%	High ÷ Low	1.100	

* Not as yet available.

TABLE 10

TEST RESULTS, TITANIUM ALLOY 5% Al, 2-1/2% Sn, STANDARD INTERSTITIAL, ANNEALED

SUMMARY OF TEST RESULTS							
Test Condition	Ultimate Tensile Strength (F_{tu} in psi)	Tensile Yield Strength		Tensile Notch Strength		Elongation in 1/2" (4 Diameters), %	Reduction of Area, %
		F_{ty} in psi	% of Ultimate Tensile	F_{tu} in psi	% of Unnotched		
Room Temperature, Unirradiated	122,900	112,900	92	166,900	136	24	48
30°R, Unirradiated	223,600	215,600	96	251,100	112	15	23
30°R, Irradiated to 1×10^{17} nvt	247,500	212,700	86	274,700	111	*	*

TEST RESULTS, 30°R, IN-PILE					
Specimen	Test Condition	Ultimate Tensile Strength (F_{tu} in psi)	Tensile Yield Strength (F_{ty} in psi)	Elongation in 1/2" (4 Diameters), %	Reduction of Area, %
Tensile Test					
3 Aa 52	1×10^{17} nvt	221,000	212,000	*	*
3 Aa 57	1×10^{17} nvt	265,000	214,000	*	*
3 Aa 58	1×10^{17} nvt	256,600	212,000	*	*
Average		247,500	212,700	*	*
Scatter		±8.9%	±1/2%		
Tensile Notch Test					
3 Aa 13	1×10^{17} nvt	283,000	Ratio, Notched-Unnotched		
3 Aa 40	1×10^{17} nvt	265,000			
3 Aa 47	1×10^{17} nvt	276,000	Avg ÷ Avg	1.11	
Average		274,700	Low ÷ High	1.00	
Scatter		±3.8%	High ÷ Low	1.28	

* Not as yet available.

4.2 DATA RECORDING

The X-Y plotter which records the dynamometer and extensometer signals to form a stress-strain curve was modified during this reporting period to partially overcome the limitations noted in Quarterly Report No. 12. As noted in Quarterly Report No. 12, Section 4.2, Page 29, the equipment is not capable of recording strain after some 2% total strain. In modifying the equipment to plot fluxuations in stress rate during the plastic deformation of samples under test, the recorder was equipped with a switching system to allow the X plot to be time actuated after strain is no longer recorded. This provides a composite curve composed of a stress-strain diagram to some 2% total strain, including the yield point, above which is a stress-time plot extending to the point of failure. Changes in the stress time slope will locate and record stress levels at the point of dislocation interactions which cause the non-linearity of the stress-strain relationship during plastic behavior as well as ensure accurate recording of the fracture stress in instances where this parameter exhibits a significant variation from ultimate tensile stress.

4.3 DATA EVALUATION

Testing has been completed for sets of at least three samples at room temperature, at $30^{\circ}R$ and at $30^{\circ}R$ explosed to 1×10^{17} nvt fast (>0.5 Mev) neutron dose for four of the thirty-three materials authorized by Contract NASw-114. These are Stainless Steels AISI Type 347 and 304 and Titanium Alloys 55A and 5% Al, 2-1/2% Sn.

4.3.1 Test Results, Stainless Steels AISI Type 304 Annealed and AISI Type 347 Annealed

The results of in-pile testing of AISI Type 304 and AISI Type 347 are given in Tables 6 and 7. A summary of the results for all test conditions for AISI 304 and AISI 347 is given in Table 8.

4.3.1.1 Cryogenic Effects

Comparison of the test results of these austenitic stainless steels at room temperature shows similar mechanical properties with the lower yield strength and greater ductility of AISI Type 304 attributable in a large part to the significant difference in grain size of the two materials. The AISI Type 304 has an ASTM grain size of 5 to 6 compared to 9 to 10 for the AISI 347, both measured in accordance with the American Society for Testing Materials Standard 112-58T. The greater density of grain boundaries in the finer grained material provides more barriers to slip and increases dislocation pile-ups along the slip planes. This increases the required stress in the early stages of plastic deformation and limits the amount of strain occurring as permanent set during this period.

Comparison of the test results for the two steels at 30°R, unirradiated, reveals a significant difference in cryogenic behavior between AISI Types 304 and 347. While the net changes in ultimate tensile strength and tensile yield strength from room temperature to 30°R were comparable (in the order of a 150% increase in ultimate, 16% increase in yield), the AISI Type 304 showed a much greater decrease in ductility parameters than AISI Type 347 and also developed a noticeable degree of notch sensitivity. AISI Type 347 also showed a reduction in ductility and in the notched/unnotched tensile strength but at a considerably less marked degree.

The mechanical properties of austenitic stainless steels at cryogenic temperatures are governed by two structural configurations; the original austenitic face-centered cubic lattice and martensite formed from the lattice during plastic deformation at cryogenic temperatures through the absorption of transformation energy from the applied load. The initial martensitic transformation product seems to be to a hexagonal close-packed lattice structure which, in the absorption of additional energy, is transformed in part to a body-centered tetragonal structure. The principal locus of transformation would be expected to occur in the grain boundary area where the transition layer of lattice atoms have less thermodynamic stability.

The presence of the brittle transformation products has the effect of increasing notch sensitivity and decreasing ductility to a degree greater than would be encountered in a stable face-centered cubic lattice. The magnitude of the effect would be a function of the volume of the transformation product formed during stressing; conditions which increase austenitic stability reduce the volume of martensite formed and so decrease the change in ductility and notch sensitivity encountered at cryogenic temperatures.

The samples of AISI Type 347 tested had appreciably higher nickel and manganese contents than the AISI 304. The increased austenitic stability provided by these elements is evident in the reported test results. It is worthy of note that the largest difference between the test data for AISI 304 and AISI 347 is in the net change of reduction of area. Reduction of area is the most structure-sensitive parameter measurable in a tension test. Therefore, it is influenced most by the degree of partial phase transformation. The wide scatter in the tensile notch sample of 304 is also attributed to a phase transformation effect.

The major cryogenic hardening effect in the original austenitic grains is due to the change in energy required to produce stacking faults during deformation. In face-centered cubic materials, a stacking fault may be considered as a sub-microscopic region of hexagonal close-packed structure bounded by partial dislocations and acting as an extended dislocation. The width of the sub-structure, a function of stacking fault energy, governs the rate of strain hardening. Since the stacking fault energy variation between AISI Type 304 and AISI Type 347 is small, the cryogenic effect on the ultimate tensile strength was similar for the two materials.

The change in tensile yield strength in these austenitic alloys is relatively minor. Both of the principal mechanisms of cryogenic hardening occur during plastic deformation and have little influence on the elastic behavior of the material. A major portion of the increase in yield strength observed occurs during the plastic portion of the curve between the modulus slope and 0.2% offset strain. Confirmation of this model of cryogenic hardening is given by the observed fact that the stress required to impart a given set in the vicinity of the yield strength increases by a factor from three to five at 30°R.

4.3.1.2 Radiation Effects

A comparison of the test data taken at 30°R, unirradiated, and at 30°R, irradiated, presents the picture of a different hardening mechanism. Both austenite stainless steel alloys exposed to a fast neutron field developed slightly higher (in the order of 6-9%) ultimate tensile strength accompanied by a somewhat greater (in the order of 20-25%) increase in tensile yield strength. There is an observable tendency towards reduction in ductility parameters, but the magnitude is within the probable range of experimental uncertainty.

The increase noted in the yield to tensile strength ratios indicates that the radiation hardening effect influences elastic behavior to a greater degree than cryogenic hardening.

The effects of radiation observed in AISI Type 304 and AISI Type 347 are not such as would impair their usefulness as engineering alloys. Both alloys were tested in only the annealed condition. Caution should be exercised in extrapolation of these test results to cold worked material or in the "as welded" condition.

4.3.2 Titanium Alloys, 55A and 5% Al, 2-1/2% Sn

Sets of three tensile and three tensile notch tests were run on each of these alpha titanium alloys. The results of these tests, with the exception of the ductility parameters which are not as yet available, are given in Tables 9 and 10 together with a summary of test results for the unirradiated samples at room temperature and at 30°R previously reported.

4.3.2.1 Cryogenic Effects

Comparison of the room temperature test results with the unirradiated 30°R test results shows that while Alloy 55A exhibits a greater net change in both tensile and yield strengths (168% and 127% versus 80 and 90%, respectively) than 5% al, 2-1/2% Sn, the yield to tensile strength ratio increases for 5% Al, 2-1/2% Sn, and decreases for 55A. This change is accompanied by a greater decrease in ducility for the 5% Al, 2-1/2% Sn, alloy. This difference in cryogenic effect is caused by the difference in chemical composition. Titanium 55A is essentially commercially

pure titanium with a total impurity content of less than 1%, approximately a third of which are interstitials. In the annealed condition, 55A has a relatively unperturbed hexagonal close-packed structure with very few randomly scattered foreign atoms.

Titanium 5% Al, 2-1/2% Sn is an essentially homogenous substitutional solid solution of aluminum and tin in alpha titanium. The presence of an appreciable number of "foreign" solute atoms in the hexagonal close-packed lattice, with atomic volumes which differ from those of the solvent atoms, provide loci for dislocation pinning, increasing the stress required to cause movement of the dislocation within the grain. This effect is particularly noticeable at the onset of plastic behavior and accounts for the increase in yield strength and reduction of ductility parameters. Apparently the effect is intensified at cryogenic temperatures, resulting in the increase in yield to tensile strength ratio and the decrease in elongation and reduction of area values reported in Table 10 for tests at 30°R.

4.3.2.2 Radiation Effects

Examination of the results of tests for irradiated specimens, compared with the unirradiated samples tested at 30°R, show an irradiation induced increase in tensile strength of 14% for 55A and 10% for 5% Al, 2-1/2% Sn. The yield strength of 55A increased some 9%; the net change in yield strength in 5% Al, 2-1/2% Sn of -1-1/3% is within the limits of probable experimental uncertainty and is not a reliable indication of a reduction in this parameter. Notch sensitivity was virtually unaffected. Although ductility parameters are not as yet available, examination of the yield to tensile strength ratios indicate that serious deterioration in this property is unlikely.

The irradiation effects observed in the titanium alloys are not such as would impair their usefulness as engineering alloys.

5 ERRATA

The curve published as Figure No. 8, in Quarterly Report No. 12, was found to be in error after distribution had been made.

The curve has been replotted with proper coordinates and new points and is published herein as Figure 6.